A new model of self-excited induction generator to feed a single phase load with an application in lighting animal farm

Nassim Ahmad Iqteit*

Electrical Engineering Department,
Kocaeli University,
Kocaeli, Turkey
Email: nassimiqteit@gmail.com
*Corresponding author

Abdel-Karim Daud

Electrical Engineering Department,
Palestinian Polytechnic University (PPU),
Palestinian, P.O. Box 198, Hebron, Palestine
Email: daud@ppu.edu

Abstract: This paper presents a new model of self-excited single-phase induction generator, used by a three-phase machine for lighting animal farm through biogas energy. The designs and applications of the previous generator models have been found to be very complex, for this reason simple and effective model of SEIG is proposed. The transient equations of the proposed model were represented by SIMULINK blocks, while the steady state equations by electrical equivalent circuit. The model is derived from Steinmetz connection circuit, stationary reference frame *qd*-axes theory and symmetrical component theorem. Experimental and simulation using MATLAB are the two methods used to prove the validity of the present model. Results obtained from the two methods were closed to each other. Also, the perfect balance point was achieved at unity power factor. This application proved that the output voltage and current have sinusoidal waves which implying that the generator was operating efficiently.

Keywords: self-excited induction generator; SEIG; biogas engine; lighting animal farm; dynamic model; steady state model.

Reference to this paper should be made as follows: Iqteit, N.A. and Daud, A-K. (2019) 'A new model of self-excited induction generator to feed a single phase load with an application in lighting animal farm', *Int. J. Power and Energy Conversion*, Vol. 10, No. 1, pp.32–50.

Biographical notes: Nassim Ahmad Iqteit graduated in Industrial Automation Engineering from the Palestine Polytechnic University (PPU), Hebron, Palestine in 2006. He received his Master's in Electric Power Engineering from the Yarmouk University, Irbid, Jordan in 2011. Currently, he is a PhD candidate in Electrical Power Engineering at the Kocaeli University, Kocaeli, Turkey. He worked in Electrical Engineering Department in PPU. His research field includes motor drives, induction generator, power system analysis and optimal size, and location of distribution generators in distribution networks.

Abdel-Karim Daud received his Master degree in Electrical Engineering from TU Dresden, Germany in 1983 and PhD from TU Berlin in 1990. He was the Director Academic Affairs, Dean of Applied Professions College and Head of Electrical Engineering Department at the Palestine Polytechnic University (PPU), Hebron/Palestine, for many years. Since January 2015, he works as Professor and currently Head of Electrical Engineering Department of PPU. He has published several papers in international journals and conferences. He has a great experience in research projects. His main research interests are electrical machines, electric drives, energy conversion, and renewable energy.

This paper is a revised and expanded version of a paper entitled 'Design a stand-alone generating system to lighting animal farm using self excited induction generator' presented at Third International Conference on Energy and Environmental Protection in Sustainable Development (ICEEP III), Hebron, West bank, State of Palestine, 9–10 October 2013.

1 Introduction

Renewable energy sources such as biogas, biomass, small hydro, wind, etc., are typically located in isolated areas devoid from utility supply. Electricity can be supplied to such remote and isolated areas through the development of autonomous, small-scale power generation system based on renewable energy. Squirrel cage induction machines are usually implemented to generate electrical power from renewable energy resources, such as wind energy and biomass. This is due to the advantages of induction generators over others types of generators. The main advantages include brushless construction, reduced size, absent of DC power supply for excitation, reduced maintenance cost, inherent short circuit protection capability and better transient performance (Gunawan et al., 2015; Barara et al., 2014; Canale et al., 2009; Mahato et al., 2008).

Most of the loads fed by the renewable energy sources such as Pico or Micro power systems are single-phase loads (Murthy et al., 2008). However single-phase induction motor can be operated as self-excited induction generator (SEIG), which is only limited to relatively small power output. Power ratings above 3 kW, three-phase induction machines are cheaper and more readily available with higher efficiency compared to equivalent sized single-phase machine and may be used for single-phase power generation (Kumar and Sharma, 2013; Mahato et al., 2007b). However, the use of three-phase SEIG for supplying single-phase loads is an extreme case of unbalanced operation, causing additional losses in the equipment due to the flow of negative sequence current component. Under these conditions, a three-phase machine would have to be de-rated in order to keep the temperature of the machine within allowable limits. Therefore, it is better to evaluate a single phase load that can be placed on the three-phase SEIG while maintaining the phase currents of the generator as balanced as possible (Shilpakar et al., 1998).

Mahato et al. (2006) studied the transient performance of a star-connected SEIG with three capacitors: parallel capacitor with load and two equal series capacitors between two phases of SEIG. The performance of the generator feeding a dynamic load was also studied in this publication. Jain et al. (2002) and Barara et al. (2014) presented generalised dynamic model of delta-connected three-phase SEIG feeding three phase

lines, with balance and unbalance excitation capacitors. Mahato et al. (2007a) presented dynamic model of three-phase IM with delta connected subjected to single phase loading with one shunt and one series excitation capacitor scheme for both resistive and inductive loads. The authors used a hybrid dynamic models for generator, stator in *abc* model and rotor in *dq* model. Chan and Lai (2001) presented a steady state performance of a delta-connected standalone three phase SEIG, with unbalanced capacitors and unbalanced loads. They used the method of symmetrical components to determine the input impedance. In another study by Chan and Lai (2005), they used the method of symmetrical components for steady state performance of three-phase SEIG feeding single phase load. The model consisted of two excitation capacitors and a current injection transformer.

According to previous literature reviews, generators models in theirs applications and designs have been found to be very complex. To mitigate that issue, a simple and suitable SEIG model to feed a single phase load was the main target of this paper. To confirm the validity of the model; a new biogas generating system was designed; and the perfect balance load was found. Figure 1 shows the design of a standalone generating system for lighting animal farm presented in this paper. This system includes three essential parts: biogas plant, SEIG system, and fixed electric load. The biogas plant consists of digester, gas holder, mixing chamber, chamber expansion, control valve, and biogas engine. The digester chamber is important part in the biogas plant and it is used to digest the dung of cattle and animals to produce the biogas for feeding engine and driving SEIG with constant speed. Biogas production is obtained by anaerobic decomposition (absent of O_2) of dung of cattle, feedstock or Poultry manure in presence of bacteria. The main process steps of biogas formation are hydrolysis, acid genesis, acetogenesis, and methanogenesis. The output biogas which is in the gas holder is mainly composed of 60% methane and 35% CO_2 and about 5% of H_2, N_2, O_2, ammonia, and moisture. The control valve is used to control the biogas pressure and flow. The calorific value of biogas is about 6 kWh/m^3 and this corresponds to about half litre of diesel oil. The net calorific value depends on the efficiency of the burners or devices. Methane is the essential component under the aspect of using biogas as a fuel. The biogas engine needs about 0.6 m^3 of biogas to produce 1 kWh.

Diesel engines can be modified to operate on biogas in two different ways, that is, dual fuel operation with ignition by pilot fuel injection and operation on gas alone with spark ignition. The power and torque characteristic of modified engine (biogas engine) is displayed in Figure 3. Approximately, the engine has a linear characteristic between torque and speed around rating values (GTZ, 1988; Seadi et al., 2008). Most lighting loads in animal farms are frosted bulbs and fluoro tubes. If this load is single phase, the three phase SEIG can supplied electric energy to it without any dangerous effects on the operation of machine or the load.

In the present work, the generalised machine theory with the help of symmetrical components theory was utilised to derive the general dynamic model of three phase SEIG, feeding single phase load with C-2C configuration. The generator's dynamic equations are given in stationary *qd* reference frame. The steady-state model was derived using the dynamic equations, with the help of admittance-based model. Nonlinear equations with unknown variables, such as output frequency and magnetising reactance were obtained. MATLAB was used to solve this nonlinear problem. The steady-state performance under different operating condition was evaluated based on the generator's

steady state mathematical model, positive and negative equivalent circuits. The Simulink/MATLAB software utilising solver ode45 was used to obtain the simulation results for transient model of the generator.

Figure 1 Biogas generating system for lighting animal farm using self excited induction generator

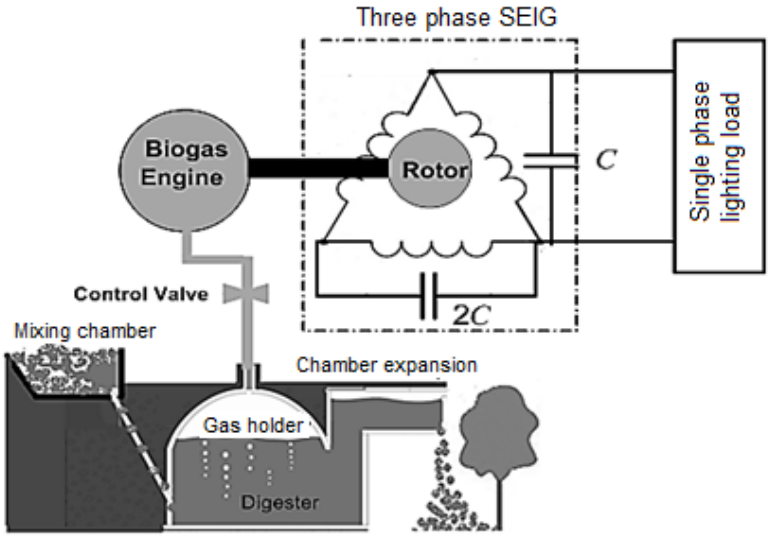

1.1 List of symbols

B	susceptance
C	capacitance
E_g	internal generated voltage
F	per unit frequency f / f_{base}
f	frequency
i_C, i_{2C}	current through capacitances
i_l	load current
i_l^s	load current at stationary reference frame
$i_{qr}^{s'}$, $i_{dr}^{s'}$	d-axis and q-axis components of rotor currents referred to stator
i_{qs}^s, i_{ds}^s	d-axis and q-axis components of stator currents
i_M	magnetising current
i_{Md}, i_{Mq}	d-axis and q-axis components of magnetising currents
i_{as}, i_{bs}, i_{cs}	stator phase currents in a, b, c phases

I_{ps}, I_{ns} positive and negative sequence components of stator phase currents

I^s_{qs}, I^s_{ds} RMS stator currents in *q*-*d* axis at stationary reference frame

J moment of inertia

j imaginary number $\sqrt{-1}$

n engine speed in rpm

p number of poles

P_{out} output power

q^s_{qs}, q^s_{ds}, q^s_l charges of excitation capacitors of stationary reference frame

s slip

R, L, X load resistance, inductance and reactance, respectively

r_s, $\acute{r}_r$ per phase stator and rotor (referred to stator) resistances

T_e developed electromagnetic torque

T_{Shaft} shaft torque of prime mover

t transpose

v_{as}, v_{bs}, v_{cs} stator voltages of *a*, *b*, *c* phases

v^s_{qs}, v^s_{ds} stator voltages in q-d axis at stationary reference frame

$v^{\acute{s}}_{qr}$, $v^{\acute{s}}_{dr}$ rotor voltages in q-d-axis referred to stator side of stationary reference frame

x_{ls}, x'_{lr} per phase stator and rotor (referred to stator) leakage inductances

x_M magnetising reactance

Y_l admittance load

Y_p, Z_n positive and negative admittance of induction machine

Y_T total admittance

Z_p, Z_n positive and negative sequence components of generator impedance

γ per unit speed ω / ω_{base}

μ voltage unbalance factor

ψ flux linkages per second

ψ^s_{qs}, ψ^s_{ds} *q* and *d* flux linkages per second for stator winding of stationary reference frame

ψ'^s_{qr}, ψ'^s_{dr} *q* and *d* flux linkages per second for rotor winding referred to stator side of stationary reference frame

ω_b base speed

ω_e electrical speed

ω_r rotor speed.

2 Mathematical model

The present model was limited to the following assumptions: prime-mover at constant speed, generator excited by two capacitors (C and 2C), load at RL load and three conditions of induction machine including:

1 equal leakage reactance of stator and rotor

2 ignored space harmonics in air-gap

3 negligible zero sequence components of stator and rotor voltages.

Based on these assumptions the dynamic model and steady state equivalent circuit of SEIG were derived.

2.1 Dynamic model

The circuit diagram of three-phase SEIG configured with two shunt capacitors excitation is shown in Figure 2.

Figure 2 Three-phase SEIG with C-2C excitation feeding power for single-phase load

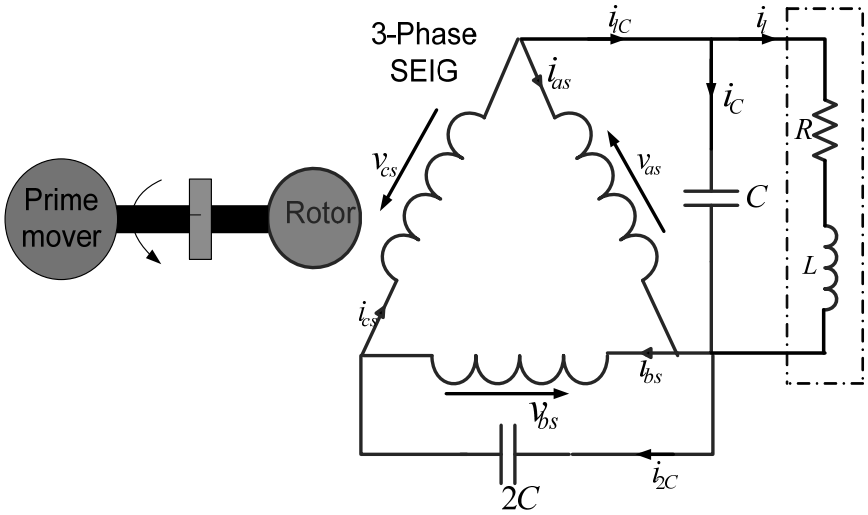

The basic terminal equations of the present configuration are given as:

$$i_{lc} = i_c + i_l \tag{1}$$

$$i_{as} - i_{bs} = 2C\frac{dv_{bs}}{dt} - C\frac{dv_{as}}{dt} - i_l \tag{2}$$

$$i_{bs} - i_{cs} = -2C\frac{dv_{bs}}{dt} \tag{3}$$

$$i_{cs} - i_{as} = C\frac{dv_{as}}{dt} + i_l \tag{4}$$

$$v_{as} = Ri_l + L\frac{di_l}{dt} \tag{5}$$

$$v_{as} + v_{bs} + v_{cs} = 0 \tag{6}$$

The dynamic model of the three-phase squirrel cage induction generator was developed by using stationary *q-d* axes reference frame (Ong, 1997) and the relevant voltage and current equations are given as:

$$[\boldsymbol{V}] = [\boldsymbol{r}][\boldsymbol{i}] + \frac{1}{\omega_b} p[\boldsymbol{\psi}] + \frac{\omega_r}{\omega_b}[\boldsymbol{G}][\boldsymbol{\psi}] \tag{7}$$

$$[\boldsymbol{\psi}] = [\boldsymbol{x}][\boldsymbol{i}] \tag{8}$$

where

$$[\boldsymbol{V}] = \begin{bmatrix} v_{qs}^s & v_{ds}^s & v_{qr}^{\acute{s}} & v_{dr}^{\acute{s}} \end{bmatrix}^t$$

$$[\boldsymbol{\psi}] = \begin{bmatrix} \psi_{qs}^s & \psi_{ds}^s & \psi_{qr}^{\acute{s}} & \psi_{dr}^{\acute{s}} \end{bmatrix}^t$$

$$[\boldsymbol{r}] = diag\begin{bmatrix} r_s & r_s & \acute{r}_r & \acute{r}_r \end{bmatrix}$$

$$[\boldsymbol{G}] = \begin{bmatrix} 0 & 0 & 0 & 0 \\ 0 & 0 & 0 & 0 \\ 0 & 0 & 0 & -1 \\ 0 & 0 & 1 & 0 \end{bmatrix}$$

$$[\boldsymbol{V}] = \begin{bmatrix} v_{qs}^s & v_{ds}^s & v_{qr}^{\acute{s}} & v_{dr}^{\acute{s}} \end{bmatrix}^t$$

$$[\boldsymbol{x}] = \begin{bmatrix} x_{ls} + x_M & 0 & x_M & 0 \\ 0 & x_{ls} + x_M & 0 & x_M \\ x_M & 0 & x'_{lr} + x_M & 0 \\ 0 & x_M & 0 & x'_{lr} + x_M \end{bmatrix}$$

and $p = (d / dt)$ is a time derivative operator.

The variables in *abc* reference frame can be transformed to *qd*0 variables by using equation (9).

$$\begin{bmatrix} f_q \\ f_d \\ f_0 \end{bmatrix} = \frac{2}{3}\begin{bmatrix} 1 & -\frac{1}{2} & -\frac{1}{2} \\ 0 & -\frac{\sqrt{3}}{2} & \frac{\sqrt{3}}{2} \\ \frac{1}{2} & \frac{1}{2} & \frac{1}{2} \end{bmatrix}\begin{bmatrix} f_a \\ f_b \\ f_c \end{bmatrix} \tag{9}$$

where the variable f may indicates voltage, currents, or flux linkage.

Expressing equations (2) to (4) in terms of *q-d* variables, the voltage equations of three-phase SEIG in terms of excitation capacitor voltages can be written as:

$$[\boldsymbol{V}] = [\boldsymbol{E}][\boldsymbol{q}] \tag{10}$$

$$[\boldsymbol{q}] = \int [\boldsymbol{i_L}]dt \tag{11}$$

where

$$[\boldsymbol{q}] = \begin{bmatrix} q_{qs}^s & q_{ds}^s & q_l^s \end{bmatrix}^t$$

$$[\boldsymbol{i_L}] = \begin{bmatrix} i_{qs}^s & i_{ds}^s & i_l^s \end{bmatrix}^t$$

$$[\boldsymbol{i}] = \begin{bmatrix} -\frac{3}{2C} & \frac{\sqrt{3}}{2C} & -\frac{1}{C} \\ \frac{\sqrt{3}}{2C} & -\frac{3}{2C} & \frac{1}{\sqrt{3}C} \\ 0 & 0 & 0 \\ 0 & 0 & 0 \end{bmatrix}$$

Assuming that the *qs*-axis is aligned with the as-axis ($v_{as} = v_{qs}^s$), the load voltage equation (5) can be rewritten by:

$$v_{qs}^s = Ri_l^s + Lpi_l^s \tag{12}$$

It is important to note that the dynamic equations deal with nonlinear magnetising inductance due to saturation, which must be suitably incorporated. This requires determination of nonlinear variation of the magnetising reactance x_M with exciting current i_M. Careful and accurate measurements of the machine by conducting synchronous speed test yielded this result (refer to Appendix). At each computation step, the magnetising current is calculated as:

$$i_M = \frac{\sqrt{i_{Mq}^2 + i_{Md}^2}}{\sqrt{2}} \tag{13}$$

where $i_{Mq} = i_{qs}^s + i_{qr}^{\acute{s}}$, $i_{Md} = i_{ds}^s + i_{dr}^{\acute{s}}$ are direct and quadrature axes components of the magnetising current space vector. The magnetising reactance is calculated from nonlinear function of i_M which describes the magnetising characteristic between x_M and i_M.

The torque balance equation of mechanical motion of the SEIG is defined as:

$$T_{shaft} = T_e + J\left(\frac{2}{P}\right)p\omega_r \tag{14}$$

where T_e is the developed electromagnetic torque which can be expressed as:

$$T_e = \frac{3P}{4\omega_b}\left(\psi_{ds}^s i_{qs}^s - \psi_{qs}^s i_{ds}^s\right) \tag{15}$$

Biogas engine power output P_{out} and torque T_{Shaft} as a function of engine speed n are given in Figure 3 (GTZ, 1988). The approximated shaft torque T_{Shaft} of prime-mover of biogas engine and speed is represented by a linear curve given as:

$$T_{shaft} = k_1 - k_2\omega_r \tag{16}$$

where T_{shaft} is the shaft torque which shows the characteristic of prime-mover; and k_1 and k_2 are constants. J is the moment of inertia of the induction machine including the machine (prime-mover) coupled on its shaft.

Figure 3 Biogas engine power output P_{out} and torque T_{Shaft} as a function of engine speed n

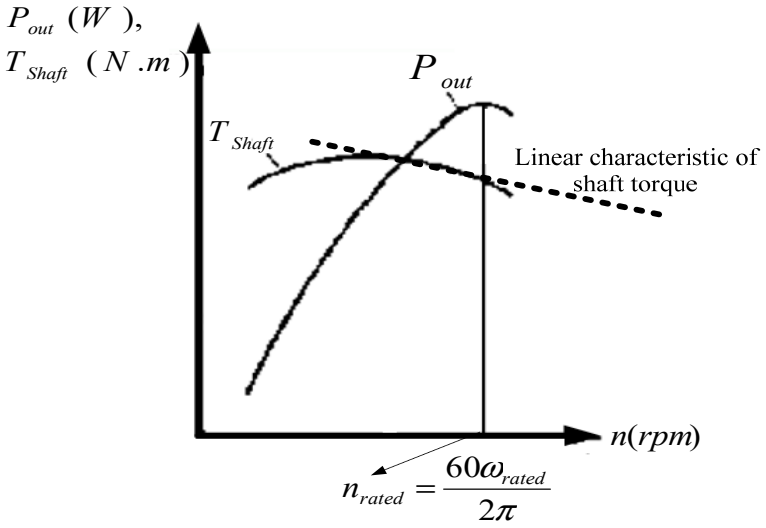

Equations (7), (11), (12) and (14) can be written in the derivative form as:

$$\left\{\begin{array}{c} p[\boldsymbol{\psi}] = \omega_b\left([\boldsymbol{V}] - [\boldsymbol{r}][\boldsymbol{i}] - \frac{\omega_r}{\omega_b}[\boldsymbol{G}][\boldsymbol{\psi}]\right) \\ p[\boldsymbol{q}] = [\boldsymbol{i_L}] \\ pi_l^s = \frac{1}{L}\left(v_{qs}^s - Ri_l^s\right) \\ p\omega_r = \frac{P}{2J}\left(T_{shaft} - T_e\right) \end{array}\right\} \tag{17}$$

Hence, these nine differential equations, given in equation (17) describe the dynamic model for the prediction of transient performance of the three-phase SEIG for single-phase power generation feeding resistive and inductive loads using C-2C configuration.

2.2 Steady state model

Positive and negative sequence equivalent circuits of three-phase SEIG feeding a single phase load at rated frequency are given in Figure 4 (Chapman, 1985), respectively.

Figure 4 (a) Positive sequence equivalent circuits and (b) negative sequence equivalent circuits of three-phase SEIG feeding a single phase load at rated frequency

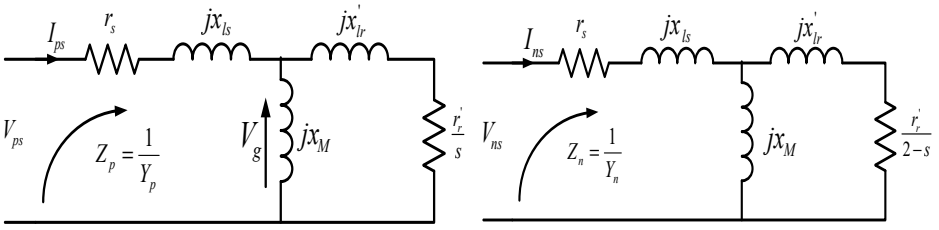

From Figure 4, the following equation can be obtained;

$$\begin{bmatrix} I_{ps} \\ I_{ns} \end{bmatrix} = \begin{bmatrix} Y_p & 0 \\ 0 & Y_n \end{bmatrix} \begin{bmatrix} V_{ps} \\ V_{ns} \end{bmatrix} \tag{18}$$

Under steady state condition, the derivative operator $(p = \frac{d}{dt})$ and the integrator operator of a variable which is varying sinusoidally at angular frequency ω_e can be given by $j\omega_e$ and $\frac{1}{j\omega_e}$, respectively (Ong, 1997).

The excitation capacitor voltages in equation (10) and the load current equation in equation (12) under steady state can be given by:

$$\begin{bmatrix} V_{qs}^s \\ V_{ds}^s \end{bmatrix} = \frac{1}{j\omega_e} \begin{bmatrix} -\frac{3}{2C} & \frac{\sqrt{3}}{2C} & -\frac{1}{C} \\ \frac{\sqrt{3}}{2C} & -\frac{3}{2C} & \frac{1}{\sqrt{3}C} \end{bmatrix} \begin{bmatrix} I_{qs}^s \\ I_{ds}^s \\ I_l^s \end{bmatrix} \tag{19}$$

$$I_l^s = \frac{V_{qs}^s}{R + j\omega_e L} = Y_l V_{qs}^s \tag{20}$$

Substitution equation (20) in equation (19), the following equation can be obtained.

$$\begin{bmatrix} I_{qs}^s \\ I_{ds}^s \end{bmatrix} = \begin{bmatrix} -j\omega_e C - \frac{2}{3} Y_l & -j\omega_e \frac{1}{\sqrt{3}} C \\ -j\omega_e \frac{1}{\sqrt{3}} C & -j\omega_e C \end{bmatrix} \begin{bmatrix} V_{qs}^s \\ V_{ds}^s \end{bmatrix} \tag{21}$$

The relationships between the r.m.s. time phasors of the positive and negative sequence variables (F_{qs}^{s}, F_{ds}^{s}) components and the rms time phasor variables (F_{ps}, F_{ns}) in *qd*-axis are given as:

$$\begin{bmatrix} F_{qs}^{s} \\ F_{ds}^{s} \end{bmatrix} = \frac{1}{\sqrt{3}} \begin{bmatrix} 1 & 1 \\ j & -j \end{bmatrix} \begin{bmatrix} F_{ps} \\ F_{ns} \end{bmatrix} \tag{22}$$

where F is current (I) or voltage (V).

Transforming equation (21) into positive and negative sequence components yielded:

$$\begin{bmatrix} I_{ps} \\ I_{ns} \end{bmatrix} = \begin{bmatrix} -j\omega_e C - \frac{1}{3}Y_l & -\frac{1}{\sqrt{3}}\omega_e C - \frac{1}{3}Y_l \\ \frac{1}{\sqrt{3}}\omega_e C - \frac{1}{3}Y_l & -j\omega_e C - \frac{1}{3}Y_l \end{bmatrix} \begin{bmatrix} V_{ps} \\ V_{ns} \end{bmatrix} \tag{23}$$

Usually, 'susceptance' is defined as $B = \omega_e C$. Now, subtracting equation (18) from equation (23) will result in equation (24).

$$\begin{bmatrix} 0 \\ 0 \end{bmatrix} = \begin{bmatrix} Y_p + jB + \frac{1}{3}Y_l & \frac{1}{\sqrt{3}}B + \frac{1}{3}Y_l \\ -\frac{1}{\sqrt{3}}B + \frac{1}{3}Y_l & Y_n + jB + \frac{1}{3}Y_l \end{bmatrix} \begin{bmatrix} V_{ps} \\ V_{ns} \end{bmatrix} \tag{24}$$

Figure 5 Equivalent circuit of three phase SEIG feeding single phase load at rated frequency

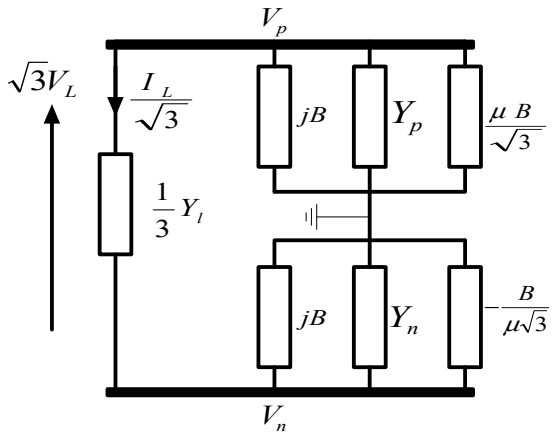

Equation (24) represents steady-state model of a three-phase SEIG feeding a single phase load. It can be rewritten to represent the equivalent circuit shown in Figure 5 in the following form:

$$\begin{bmatrix} 0 \\ 0 \end{bmatrix} = \begin{bmatrix} Y_p + jB + \frac{1}{\sqrt{3}} B\mu + \left\{\frac{1}{3} Y_l\right\} & \left\{\frac{1}{3} Y_l\right\} \\ \left\{\frac{1}{3} Y_l\right\} & Y_n + jB - \frac{1}{\sqrt{3}} \frac{B}{\mu} + \left\{\frac{1}{3} Y_l\right\} \end{bmatrix} \begin{bmatrix} V_{ps} \\ V_{ns} \end{bmatrix} \tag{25}$$

where

$$\mu = \frac{V_{ns}}{V_{ps}} = \frac{Y_p + jB + \frac{1}{\sqrt{3}} B}{Y_n + jB - \frac{1}{\sqrt{3}} B}$$

3 Experimental setup

A three-phase squirrel cage induction machine coupled with a separate excited dc motor which operates as the prime-mover was used for this experiment. The parameters and the magnetisation characteristics of the induction machine obtained by dc resistance test, block rotor test and synchronous speed test are given in Appendix.

4 Results and discussion

Three-phase squirrel cage induction machine of 1.5 kW was simulated with a 3.5 kW biogases engine which operates as the prime mover. The biogas engine included suitable control valve to provide 1,515 rpm constant-speed with different loads. The biogas engine parameters such as lighting loads values, induction generator parameters and magnetisation characteristics were obtained by conducting various tests. Those values are reported in the appendix.

The simulated performance and experimental results are presented according to three different aspects: excitation capacitors, power factors and speeds of rotation values. The experimental results obtained were compared with the simulated results to validate the developed dynamic and steady state models.

4.1 Transient analysis

Figure 6 shows the general Simulink blocks to simulate the transient mathematical model of three-phase SEIG feeding a single phase lighting load. There are four blocks. The first block represents the prime mover torque and the constants k_1 and k_2 are used to describe the torque behaviour of prime mover. The second one includes the induction generator model. The third block includes self-excited capacitors model and the fourth contains the load model. The solver ode45 in MATLAB was used to obtain the simulation results for transient model of the generator. These results include the currents and voltages of the lighting loads.

Figure 6 Transient model of SEIG with C-2C configuration feeding a single phase lighting load (see online version for colours)

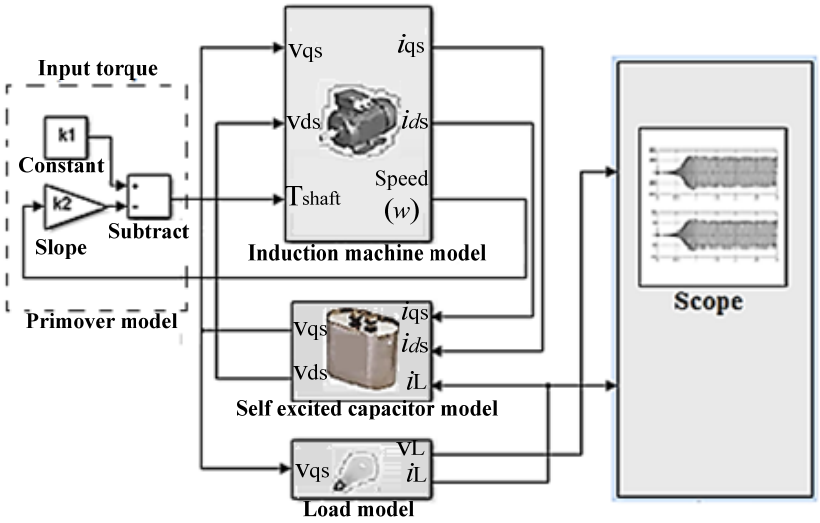

Figure 7 Load voltage and Load current: (a) C = 40 µF, Z_L = 45 Ω. P_F = 1, n = 1,515 rpm (b) C = 40 µF, Z_L = 45 Ω. P_F = 0.96 lagging, n = 1,515 rpm (c) C = 60 µF, Z_L = 45 Ω, P_F = 0.96 lagging, n = 1,515 rpm

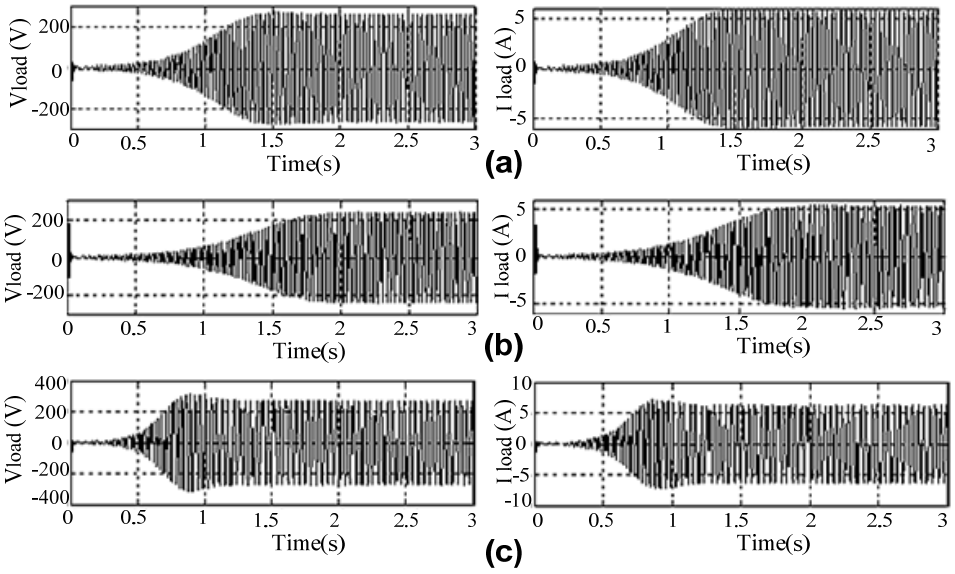

The induction generator was driven at 1,515 rpm. The simulated results for the load voltage and load current build-up as shown in Figure 7 indicated that the generator voltage remains small due to low level of the air-gap flux linkage. Thereafter, there was a rapid growth of voltage till the steady-state value became constant, due to magnetising

flux saturation. Figure 7 shows the load voltage and load current during transient and steady state periods of the generator operation. Figure 7(a) shows the voltage and current of resistive load (R_L = 45 Ω ≈ 11 frosted bulb with parallel connection). Figure 7(b) displays the voltage and current of an inductive load (Z_L = 45 Ω and P_F = 0.96 lagging; this load is equivalent to 36 of T5 fluoro tubes with parallel connection). In these cases, the loads were connected across the generator terminals by two single phase capacitors of 40 μF and 80 μF. The following results were found: the resistive load voltage and load current were respectively slightly greater than the inductive load voltage and load current, the load self-excitation voltage with resistive load took less time to build-up than the inductive load. Figure 7(c) shows the voltage and the current of inductive load (Z_L = 45 Ω and P_F = 0.96 lagging) when the generator was driven at speed of 1,515 rpm and excited by the capacitors 60 μF and 120 μF. It was also found that an increase in the excitation capacitor led to an increase in the load curves of voltage and current, and theirs build-up time also decrease at the same time.

4.2 Steady state analysis

Figures 8 and 9 were obtained by running the generator at a speed of 1,515 rpm, and using 40 μF and 80 μF excitation capacitors. The variation of the load voltage and output power with load current is shown in Figure 8. The load voltage decreased in close linear relationship with current load until the saturation took place at the edge of the unstable region. Also, the output power increased linearly with load until saturation point was reached. However, the load voltage and output power decreased together with decreasing power factor. Also, stable range of the load current decreased when power factor was decreasing. Figures 9 and 10 show the phase voltages and the phase current of the generator with respect to load current, respectively. At resistive load (P_F = 1), it can be easily observed from these two figures that, the three phase voltages and the three phase currents intersect at the specific point known as perfect balance point.

Figure 8 Load voltage and output power versus load current at different values of power factors

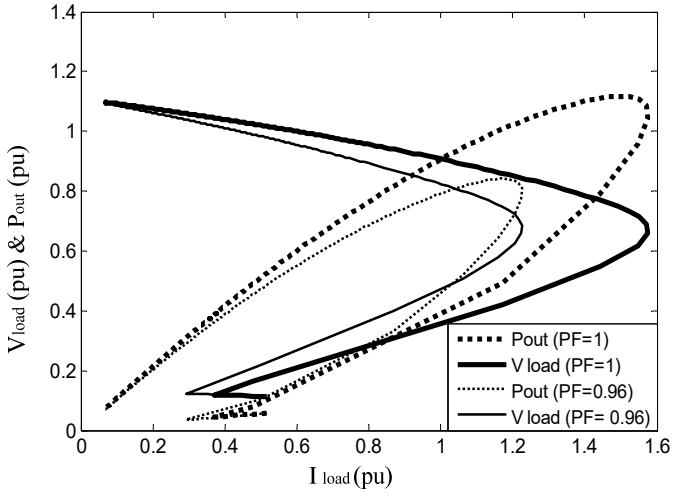

Figure 9 Phase voltages versus load current at different values of power factors

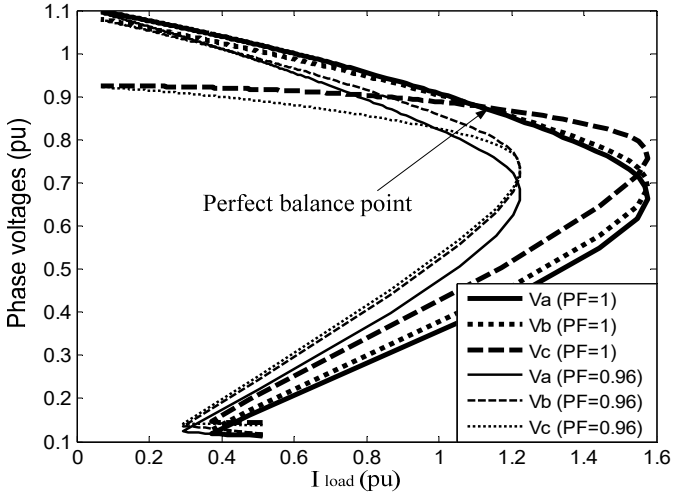

Figure 10 Phase currents versus load current at different values of power factors

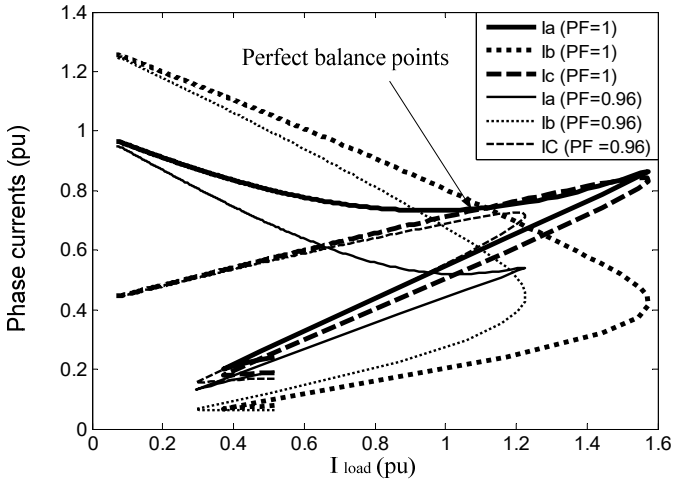

At this point of operation, the three phase voltages are equal and the three phase currents are also equal. Once the generator reaches this point, smooth operation with minimum vibrations can be easily observed. Also, from the same figures we can examine that the generator turn to lose the perfect balance point under inductive loads.

4.3 Experimental verification of SEIG model

Figures 11 and 12 and the results in Table 1 were obtained when the generator was operated at a speed of 1,150 rpm and excitation capacitors of 60 μF and 120 μF. Figure 11 shows the results of load voltage and load current during transient and steady state periods of the generator operation. Simulations showed that the load voltage and load current requires 1.25 second to build up and reach their rms values of 134.3 V and

3.25 A, respectively. Experimental results showed that, approximately the same time is needed to build up and reach rms voltage of 136.4 V and rms current of 3.2 A. A close agreement between simulation results and their practical counterpart values confirmed the validity and accuracy of the proposed transient model's analysis. The variations of the load voltage and output power with load current are shown in Figure 12. The load voltage decreased in close linear relationship with load until the saturation took place, where the region of unstable operation was reached. Similarly, the output power increased linearly with load until saturation point was attained. It was examined that the simulation results were in closed agreement with their corresponding experimental test results. Table 1 summarises the results obtained when the perfect balance point was attained.

Figure 11 On-load phase voltages at perfect balance point

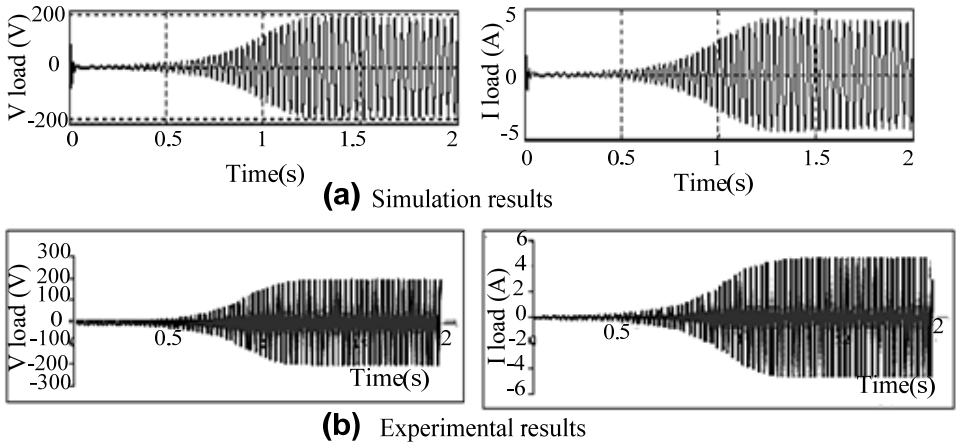

Figure 12 Variations of the load voltage and output power with load current

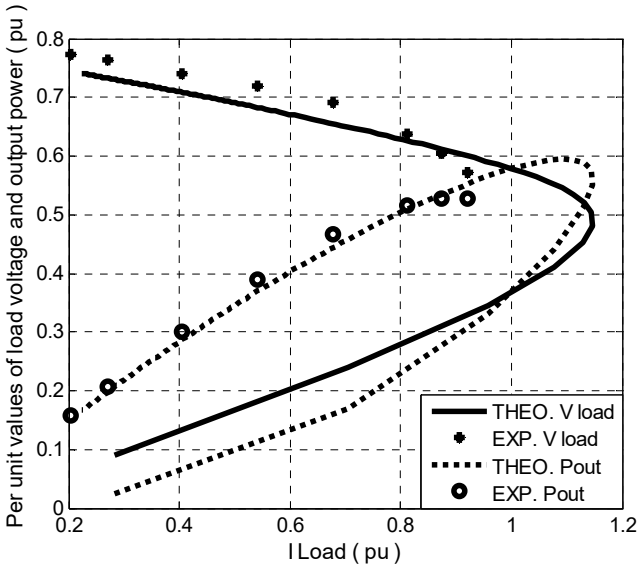

Table 1 Simulation and experimental results at perfect balance point

	C_2 (uF)	C_3 (uF)	I_L (pu)	I_{ph} (pu)	V_L (pu)
SIM.	120	60	0.8787	0.5862	0.6105
EXP.	120	60	0.873	0.568	0.605

5 Conclusions

The dynamic and steady state behaviours of SEIG feeding single phase load with C-2C capacitor excitation were studied by developing a dynamic model in the *qd* axes in stationary reference frame. Also, the generator steady state model was derived from transient model with the help of symmetrical components and admittance circuit models. Simulink and MATLAB were used to simulate the transient and steady-state models at different conditions of operation. Based on simulation results at different transient and steady state conditions, it was concluded that the approach made in the development of dynamic and steady state models is efficient.

Perfect balance point of Steinmetz configuration can be achieved when the excitation capacitors are connected in C-2C configuration and at the resistive load of the generator. The results showed that phase shift between each of the two-phase voltages is approximately 120°. The same phase shift was obtained for each of the two phase currents. This generator can be used in constant power applications, such as biogas and biomass power generation, micro-hydro power generation and wind power generation.

For the experimental results, the fairly good concordance reached between the results obtained from transient analysis and steady state analysis accurately validates the model. The results indicate that the C-2C configuration has good voltage regulation, stable excitation system and good balance operation. Also, the output voltage and current have sinusoidal waves.

References

Barara, M., Abbou, A., Ionita, S., Lefter, E. et al. (2014) 'Experimental analysis on a self excited induction generator for standalone wind electric pumping stations', *12th International Conference on Development and Application Systems*, Suceava, Romania, pp.29–36.

Canale, M., Fagiano, L. and Milanese, M. (2009) 'KiteGen: a revolution in wind energy generation', *Energy*, Vol. 34, No. 3, pp.355–361.

Chan, T.F. and Lai, L.L. (2001) 'Steady-state analysis and performance of a stand-alone three-phase induction generator with asymmetrically connected load impedances and excitation capacitances', *IEEE Trans. Energy Conversion*, Vol. 16, No. 4, pp.327–333.

Chan, T.F. and Lai, L.L. (2005) 'Single-phase operation of a three-phase induction generator using a novel line current injection method', *IEEE Trans. Energy Conversion*, Vol. 20, No. 2, pp.308–315.

Chapman, S. (1985) *Electric Machinery Fundamentals*, McGraw-Hill, New York.

Gunawan, R., Yusivar, F. and Yan, B. (2015) 'The self excited induction generator with observation magnetizing characteristic in the air gap', *International Journal of Power Electronics and Drive System (IJPEDS)*, Vol. 5, No. 3, pp.355–365.

Jain, S.K., Sharma, J.D. and Singh P. (2002) 'Transient performance of three-phase self-excited induction generator during balanced and unbalanced faults', *IEE Proceedings, Generation, Transmission and Distribution*, Vol. 149, pp.50–57.

Kumar, A. and Sharma, V.K. (2013) 'Implementation of self-excited induction generator (SEIG) with IGBT based electronic load controller (ELC) in wind energy systems', *International Journal of Research in Engineering and Technology (IJRET)*, Vol. 2, No. 8, pp.188–193.

Mahato, S.N., Sharma, M.P. and Singh, S.P. (2006) 'Transient analysis of a single-phase self-excited induction generator using a three-phase machine feeding dynamic load', *IEEE Power Electronics, Drives and Energy Systems, Conf*., pp.1–6.

Mahato, S.N., Sharma, M.P. and Singh, S.P. (2007a) 'Steady state and dynamic behavior of single-phase self-excited induction generator using a three-phase machine', *International Journal of Emerging Electric Power Systems*, Vol. 8, Art. 5, No. 3.

Mahato, S.N., Sharma, M.P. and Singh, S.P. (2007b) 'Transient performance of a single-phase self-regulated self-excited induction generator using a three-phase machine', *Electric Power System Research*, Vol. 77, No. 7, pp.839–850.

Mahato, S.N., Singh, S.P. and Sharma, M.P. (2008) 'Capacitors required for maximum power of a self-excited single-phase induction generator using a three-phase machine', *IEEE Trans. on Energy Conservation*, Vol. 23, No. 2, pp.372–381.

Murthy, S.S., Bhuvaneswari, G., Gao, S. and Gayathri, M. (2008) 'Performance analysis of a self-excited induction generator with digitally controlled electronic load controller for micro hydel power generation', in *Proc. IEEE Power System Technology and IEEE Power India Conference, Conf*., pp.1–6.

Ong, C.M. (1997) *Dynamic Simulation of Electric Machinery Using Matlab/Simulink*, Prentice Hall, London.

Seadi, T.A., Rutz, D., Prassl, H., Köttner, M., Finsterwalder, T., Volk, S. and Janssen, R. (2008) *Biogase Handbook*, Published by University of Southern, Esbjerg, Denmark.

Shilpakar, L.B., Singh, B. and Singh B.P. (1998) 'Dynamic behavior of three-phase self-excited induction generator for single-phase power generation', *Electr. Power Syst. Res*., Vol.48, pp.37–44.

Technical Cooperation (GTZ) (1988) *Biogas Plants*, German Appropriate Technology Exchange (GATE) and German Agency, Eschborn, Germany.

Appendix

Biogas engine

Single cylinder, four-stroke, force air-cooled, consumption 3.5 m^3/h biogas liquefied petroleum gas (LPG), rated output is 3.5 kW, rated speed 3,000 rpm.

Lighting loads

a frosted bulb, 100 W, 220 V, unity power factor, brightness 1,270 lumens.

b T5 fluoro tube, 30.7 W, 227V, 0.96 lagging power factor (with capacitor), 410 Lux.

The base quantities used to obtain the per-unit system's parameters

Base voltage (V_{base}) =220V, base current (I_{base}) = 3.7 A, base power (P_{base}) = 220*3.7 = 814 W, base impedance (Z_{base}) = 59.5 Ω.

Induction generator

1.5 kW, three-phase, four pole, 50 Hz, line to line voltage (V) 220Δ/380Y, line to line current (A) 6.4Δ/3.7Y, 1,415 rpm, 0.77 lagging power factor, r_s = 5.027 Ω, $\acute{r}_r$ =3.51 Ω, x_{ls} = 5.78 Ω, x'_{lr} = 5.78 Ω, x_M = 98.92 Ω. The relationship between $E_g = \frac{V_g}{F}$ and x_M, and the relation between x_M and I_M, are given by:

$$E_g = -0.1314x_M^5 + 0.7269x_M^4 - 1.4118x_M^3 + 1.1262x_M^2 - 0.6172x_M + 1.4779$$

$$x_M = 1.8324I_M^3 - 12.972I_M^2 + 8.1574I_M + 156.67$$